Syntax Literate: Jurnal Ilmiah Indonesia p–ISSN: 2541-0849
e-ISSN: 2684-883X
Vol. 6, No. 8, Agustus 2021

ANALYSIS OF SUBSOIL LIQUEFACTION POTENTIAL IN THE REGION OF MATARAM CITY IN INDONESIA

Intan Puspitaningrum
Warsaw University of Life Science, Poland
Email: intanpuspita2105@gmail.com

Abstract

One of the reasons of subsoil liquefaction are cyclical loads induced from earthquake. It generally take in the subsoil when there is a loose saturated granular soil. Loose, sand and silty sand have the highest probability of liquefaction. Most places prone to this event are the subsoil that is close to water source, namely river or bay area. Mataram city is located on the west coast of Lombok Island. It acts as the capital and economic powerhouse of the region. The 2018 M7.0 earthquake showed how devastating the earthquake effect on people's livelihood. Understanding the potential of subsoil liquefaction to happen is crucial to help government and people on the potentially affected area to adjust the proper mitigation actions. Upon analysis of soil data taken from 9 SPT sites and 22 CPT sites, it is concluded that the subsoil of Mataram city is prone to exposed with liquefaction with the most severe area is the west coast of the city and the least probable is the eastern part. Maximum settlement is forecasted to be 0.458 m taken from CPT-21 site.

Keywords: liquefaction potential, Cyclic Stress Ratio CSR, Cyclic Resistance Ratio CRR, displacement, Mataram

Introduction

The 2018 earthquake that happen on Sunday 29th of July with magnitude of M6.4 in Lombok and Bali, or to be precise on 47 km away from Lombok's capital of Mataram with epicenter on 24 km deep left a devastating effects. With reportedly a considerable amount of death toll and people suffering from injury, it is one of the strongest that ever occurred in the area. Thousands of people were left with no place to return, while infrastructure are being not functional and further threats from landslide increasing the possibility of worsening situation (Putra, Kiyono, Ono, & Parajuli, 2012).

The earthquake occurred in several series, namely foreshock (July 29th) with M6.4, main shock (August 5th) with M7.0, and aftershock (August 9th) M6.2. Lombok is surrounded by several active earthquake sources, Back Arc Thrust Zone in the north, megathrust in the south, and faults on both west and east sides (Lonteng, Balamba, Monintja, & Sarajar, 2013).

After the M7.0 mainshock, several phenomenons happen in numbers of locations scattered along the west coast to north coast of Lombok. Landslide was the

How to cite:	Puspitaningrum, Intan (2021) Analysis of Subsoil Liquefaction Potential in The Region of Mataram City in Indonesia. *Syntax Literate: Jurnal Ilmiah Indonesia* 6(8). http://dx.doi.org/10.36418/ syntax-literate.v6i8.3885
E-ISSN:	2548-1398
Published by:	Ridwan Institute

major phenomonon occurred along the west coast resulting in cut of transportation and access from the main port in west coast to the most affected area in the north. Land subsidiary and uplift were also spotted in several areas. Land subsidance was identified mostly occurred along the west coast with signs of small tsunami. Vertical uplift mainly happen on the northern part of the island, close to the epicenter with recorded number of 0.44 m higher prior to the earthquake (Saut, 2015).

Signs of liquefaction is observed on smaller scale. It happen as a result of a strong earthquake's vibration in an area with mostly containing aluvial sedimentation combined with fine particles of soil, saturated, and typically shallow groundwater depth (Lonteng et al., 2013).

Looking back at the 2018 earthquake, Mataram as the capital of Lombok acts as economic powerhouse and the most populous city in the island shall be suffering from the effects of the upcoming earthquake in the future. Therefore understanding the potential possibility of the upcoming aftermath of earthquake in the form of liquefaction is one among many things we can do to mitigate the outcome.

Methods

The aim of this research is to analyze the liquefaction potential of the subsoil of Mataram city in Lombok using the soil data taken using SPT and CPT in several locations. Soil data then being analyzed to calculate the cyclic resistance ratio (CRR) and stress ratio (CSR) in order to obtain the factor of safety (FS). For the further analysis we only use FS value from CPT result to obtain vertical (*S*) and lateral displacement (LD). CPT has become very popular for site characterization because of its greater repeatability and the continuous nature of its profile as compared with other field test (Zhang, Robertson, & Brachman, 2002). The liquefaction degree was assessed by using the Liquefaction Potential Index (I_L). Lateral displacements (LD) were also evaluated based on the known ground slope (S) and lateral displacement index (LDI).

(Warman & Jumas, 2013) did research on three locations to identified the factor of safety over the potential of liquefaction in Padang city, Sumatra on 2009 after the M7.6 tectonic earthquake. Soil investigation is done using CPT referring to ASTM D 3441-86 Standard. The result then analyzed using equation to calculate the Cyclic Stress Ratio (CSR) and Cyclic Resistance Ratio (CRR). Result shows area with relatively safe from liquefaction potential is having cone resistance (q_c) > 100 kg/cm^2 (10 MPa), and dominated by soil types of sandy silt and silty sand.

(Obermeier, 1996) also describe the term "Liquefaction potential" relates to the likelihood of liquefaction occurring during a specific earthquake at a particular strength of shaking. Even a saturated, very loose sand has no liquefaction potential if the severity of shaking is low enough. Calculation or an estimation in determining the potential of a soil to experience liquefaction requires two variables: (1) the seismic demand on a soil layer, or CSR, and (2) the capacity of the soil to resist liquefaction, expressed in Cyclic Resistance Ratio (CRR). Composed the following formula for calculation of Cyclic Stress Ratio (CSR):

$$CSR = 0.65\ (a_{max}/g)(\sigma_{v0}/\sigma'_{v0})r_d$$

Where
a_{max} = peak horizontal acceleration at the ground surface generated by the earthquake
g = acceleration of gravity
σ_{v0} = total stress
σ'_{v0} = total effective stress
r_d = stress reduction coefficient.

Accounts for the flexibility of the soil profile. (Blake, 1996) provides with approximation formula to determine the r_d value derived from the mean curve formula by and further developed by:

$$r_d = \frac{(1.000 - 0.4113\ z^{0.5} + 0.04052\ z + 0.001753\ z^{1.5})}{(1.000 - 0.4177\ z^{0.5} + 0.05729\ z - 0.006205\ z^{1.5} + 0.001210\ z^2)}$$

Where *z* is the depth beneath ground surface in meter.

As for the CRR value, several field test that are common to be used have gained evaluation of liquefied resistance, including the Standard Penetration Test (SPT), the Cone Penetration Test (CPT), shear-wave velocity measurement (Vs), and the Becker penetration test (BPT). SPT and CPT are generally preferred due to the more extensive database and experience (Tijow, Sompie, & Ticoh, 2018).

Criteria for evaluation of liquefaction resistance based on the SPT is largely constitute of CSR versus $(N_1)_{60}$ plot as shown in Figure 1. $(N_1)_{60}$ is the SPT blow count normalized to an overburden pressure of approximately 100 kPa (1 ton/sq ft) and a hammer energy ratio or hammer efficiency of 60%. Curves were made to accommodate granular soils with the fines contents of 5% or less, 15%, and 35% as shown. The CRR curve for fines contents <5% is the basic penetration criterion for the simplified procedure and is referred as “SPT clean-sand base curve”.

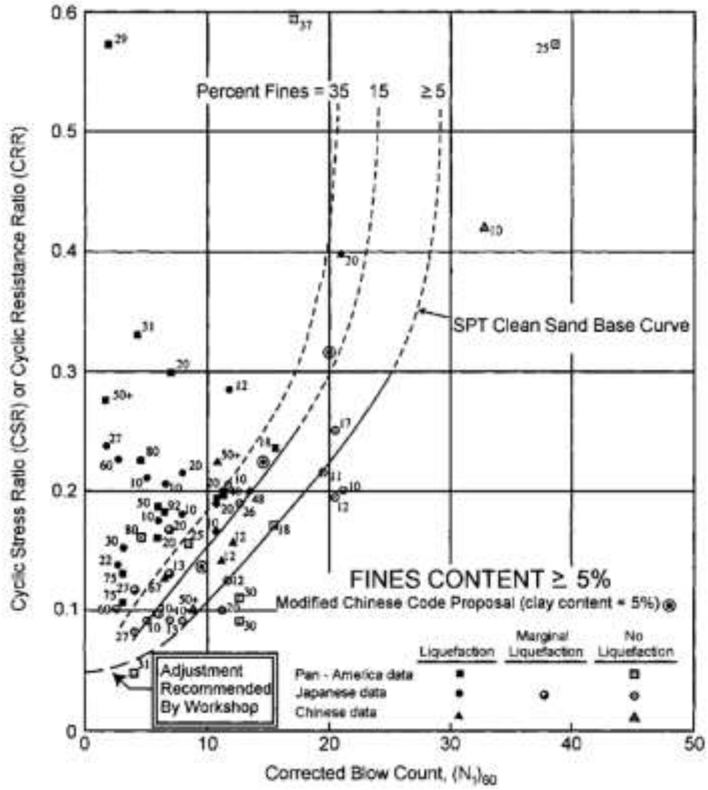

Figure 1
SPT Clean-Sand Base Curve for M7.5 earthquake with data from liquefaction history
(Source: Journal of geotechnical and geoenvironmental engineering, 2001)

Further developed an approximated formula for clean-sand base curve plotted in Figure 1 by the following equation:

$$CRR_{7.5} = \frac{1}{34 - (N_1)_{60}} + \frac{(N_1)_{60}}{135} + \frac{50}{[10\,.\,(N_1)_{60} + 45\,]^2} - \frac{1}{200}$$

The above equation valid for $(N_1)_{60} < 30$. For $(N_1)_{60} \geq 30$, clean granular soils are too dense to liquefy and are classed as non-liquefiable. (Youd & Idriss, 2001) on the Summary Report from the 1996 NCEER and 1998 NCEER workshop recommend the following formula as correction for the influence of fines content (FC) on CRR:

$$(N_1)_{60cs} = \alpha + \beta (N_1)_{60}$$

Where α and β is coefficient obtained from the following relationship:

$\alpha = 0$ for FC ≤ 5%
$\alpha = exp[1.76 - (190/FC^2)]$ for 5% < FC < 35%
$\alpha = 5.0$ for FC ≥ 35%
$\beta = 1.0$ for FC ≤ 5%
$\beta = [0.99 + (FC^{1.5}/1{,}000)]$ for 5% < FC < 35%
$\beta = 1.2$ for FC ≥ 35%

Other correction due to the additional factors involve to fines content and grain characteristics influence SPT result, as shown in Table 1. Equation below constitutes the corrections:

$$(N_1)_{60} = N_m C_N C_E C_B C_R C_S$$

Where

N_m = measured standard penetration resistance

C_N = factor to normalize Nm to a common reference effective overburden stress

C_E = correction for hammer energy ratio (ER)

C_B = correction factor for borehole diameter

C_R = correction factor for rod length

C_S = correction for samplers with or without liners

Table 1

Corrections to SPT

Factor	Equipment variable	Term	Correction
Overburden pressure	-	C_N	$(P_a/\sigma'_{v0})^{9.5}$
Overburden pressure	-	C_N	$C_N \leq 1.7$
Energy ratio	Donut hammer	C_E	0.5 – 1.0
Energy ratio	Safety hammer	C_E	0.7 – 1.2
Energy ratio	Automatic-trip Donut-type hammer	C_E	0.8 – 1.3
Borehole diameter	65 – 115 mm	C_B	1.0
Borehole diameter	150 mm	C_B	1.05
Borehole diameter	200 mm	C_B	1.15
Rod length	<3 m	C_R	0.75
Rod length	3 – 4 m	C_R	0.8
Rod length	4 – 6 m	C_R	0.85
Rod length	6 – 10 m	C_R	0.95
Rod length	10 – 30 m	C_R	1.0
Sampling method	Standard sampler	C_S	1.0
Sampling method	Sampler without liners	C_S	1.1 – 1.3

As for liquefaction analysis using CPT data, A primary advantage of using CPT is that a nearly continuous profile of penetration resistance is developed for stratigraphic interpretation. The result is generally more consistent compared to that of SPT. The stratigraphic capability of CPT makes it particularly good for assessing liquefaction-resistance profile. Figure 2 given by (Robertson, 2016) for direct determination of CRR for clean sands (FC ≤ 5%) from CPT data is valid for M7.5 earthquakes only. It shows calculated cyclic resistance ratio plotted as a function of dimensionless, corrected, and normalized CPT resistance q_{c1N} from sites where surface effects of liquefaction were or were not observed following past earthquakes (Sasmi et al., 2020).

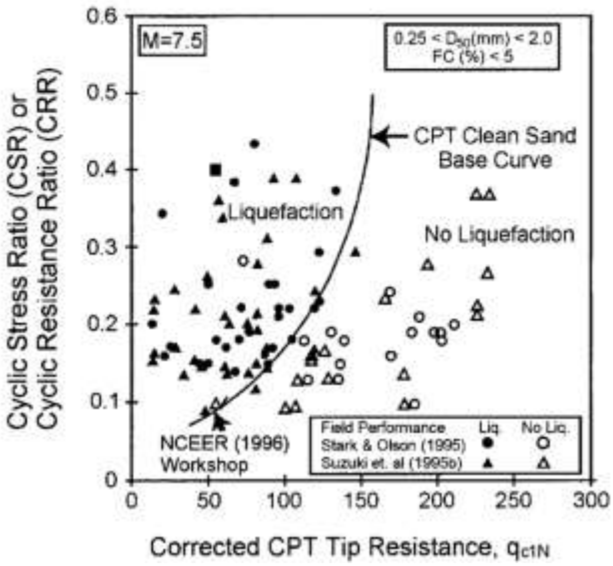

Figure 2
Recommended cyclic resistance ratio (CRR) for clean sand under level ground conditions based on CPT

The clean-sand curve at Figure 2 may be approached by the following equation (Robertson, 2016).

If $(q_{c1N})_{CS} < 50$ then $CRR_{7.5} = 0.833[(q_{c1N})_{CS}/1{,}000] + 0.05$

If $50 \leq (q_{c1N})_{CS} < 160$ then $CRR_{7.5} = 93[(q_{c1N})_{CS}/1{,}000]^3 + 0.08$

Where the $(q_{c1N})_{cs}$ is the clean-sand cone penetration resistance normalized to approximately 100 kPa (1 atm).

The CPT procedure requires normalization of tip resistance. This corrections lead to normalized, dimensionless cone penetration resistance q_{c1N}.

$$q_{c1N} = C_Q(q_c/P_a)$$

Where

$$C_Q = (P_a/\sigma'_{v0})^n$$

Where
C_Q = normalizing factor for cone penetration resistance
P_a = 1 atm of pressure in the same units used for σ'_{v0}
n = exponent that varies with soil type
q_c = field cone penetration resistance measured at the tip

(Robertson, 2016) give Figure 3 for estimation of soil type. The boundaries between soil types 2 – 7 can be approximated by concentric circles and can be used to account for effects of soil characteristics on q_{c1N} and CRR. The radius of circles, is referred as soil behavior type index I_c, is calculated by the following formula:

$$I_c = [(3.47 - \log Q)^2 + (1.22 + \log F)^2]^{0.5}$$

Where

$$Q = [(q_c - \sigma_{v0})/P_a][(P_a/\sigma'_{v0})^n]$$

and

$$F = [f_s/(q_c - \sigma_{v0})] \times 100\%$$

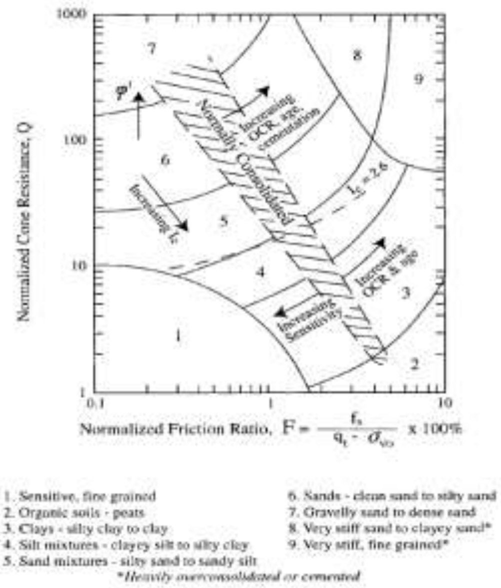

Figure 3
CPT-Based Soil Behavior-Type Chart

The soil behavior chart in Figure 3 was developed using an exponent n of 1.0, which is appropriate value for clayey soil types. However, for clean sand, an exponent between 0.5 is more appropriate, and a value between 0.5 and 1.0 would be appropriate for silts and sandy silts (Jefferies & Been, 2019). Differentiation is performed by assuming an exponent n of 1.0 (characterized as clay) and calculating the dimensionless CPT tip resistance Q from the following equation:

$$Q = [(q_c - \sigma_{v0})/P_a][P_a/\sigma'_{v0}]^{1.0} = [(q_c - \sigma_{v0})/\sigma'_{v0}]$$

If the I_c calculated with an exponent of 1.0 is >2.6, the soil is classified as clayey and is considered too clay-rich to liquefy, and the analysis is complete. If the calculated I_c is <2.6, the soil is most likely granular in nature, thus C_Q and Q should be recalculated using an exponent n of 0.5. I_c then shall be recalculated. If the recalculated Ic is <2.6, the soil is classified as non-plastic and granular. However if the I_c is >2.6, the soil is likely to be very silty and possibly plastic. In this case, q_{c1N} should be recalculated using an intermediate exponent n of 0.7 (Aryastana, Ardantha, Eka Nugraha, & Windy Candrayana, 2017).

In order to normalized penetration resistance (q_{c1N}) for silty sands is corrected to an equivalent clean sand value (qc1N) cs by (Castelli & Lentini, 2010) the following equation:

$$(q_{c1N})_{cs} = K_c q_{c1N}$$

Where K_c, the correction factor for grain characteristics, is defined by the following formula:

$$\text{for } I_c \leq 1.64 \qquad Kc = 1.0$$
$$\text{for } I_c > 1.64, \qquad K_c = -0.403 I_c{}^4 + 5.581\, I_c{}^3 - 21.63\, I_c{}^2 + 33.75\, I_c - 17.88$$

Since the clean-sand base or CRR of SPT and CPT on the above section of this chapter is only apply to magnitude 7.5 earthquakes. To adjust the clean-sand curves to magnitude smaller or larger than 7.5, (Green et al., 2017) introduced correction factors coined ‘magnitude scaling factors (MSF)’. Therefore, the equation on finding the safety factor FS of the potential of liquefaction to be happened is written as follows:

$$FS = (CRR_{7.5}/CSR)MSF$$

Where
CSR = calculated cyclic stress ratio generated by the earthquake shaking
$CRR_{7.5}$ = cyclic resistance ratio for magnitude 7.5 earthquakes

Several scaling factors are proposed by researches as provided in Table 2. For engineering practice purpose, it is recommended for magnitude <7.5 the lower bound for the recommended range is the new MSF proposed by Idriss in column 3 of Table 2.

Table 2
MSF Value Defined By Various Investigators

Magnitude (1)	Seed and Idriss (2)	Idriss (3)	Andrus and Stokoe (4)
5.5	1.43	2.20	2.8
6.0	1.32	1.76	2.1
6.5	1.19	1.44	1.6
7.0	1.08	1.19	1.25
7.5	1.00	1.00	1.00
8.0	0.94	0.84	0.8
8.5	0.89	0.72	0.65

To estimate the severity of liquefaction degree at given site, proposed the liquefaction potential index (I_L) as follows:

$$IL = \int_0^{20} F_L W(Z) dZ$$

For sites with level ground, far from any free face, it is reasonable to assume that little or no lateral displacement occur after earthquake, such that the volumetric strain will be equal or close to the vertical strain. If the vertical strain in each soil layer is integrated with depth using this equation, the result should be an appropriate index of potential liquefaction-induced ground settlement at the CPT location due to the design earthquake.

$$S = \sum_{i=1}^{j} \varepsilon_{vi} \Delta_{Zi}$$

Where

FL = $1 - FS$ for $FS \leq 1.0$ and $F=0$ for $FS > 1.0$

W (Z) = $10 - 0.5Z$ (Z in meters and the depth 20 m is decided considering where the liquefaction happen during the past earthquake phenomena)

The following simplified procedure for assessing soil liquefaction based om the IL can act as the preliminary guideline.

$I_L = 0$	Liquefaction risk is very low
$0 < I_L \leq 5$	Liquefaction risk is low
$5 < I_L \leq 5$	Liquefaction risk is high
$15 < I_L$	Liquefaction risk is very high

Where S is the calculated liquefaction-induced ground settlement; ε_{vi} is the postliquefaction volumetric strain for the soil sublayer *i* ; Δzi is the thickness of the sublayer *i*; and *j* is the number of

soil sublayers.

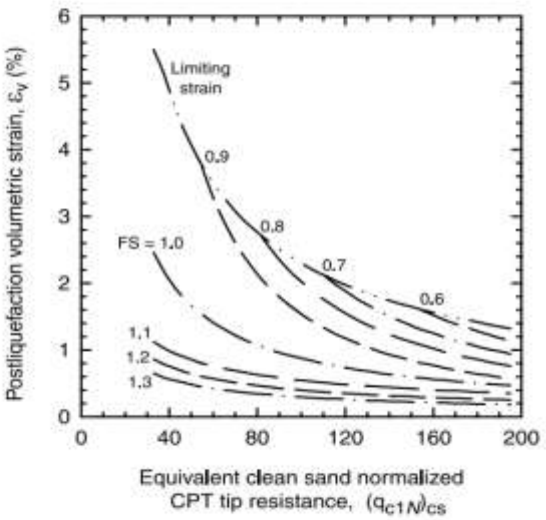

Figure 4

Relationship Between Postliquefaction Volumetric Strain and Equivalent Clean Sand Normalized CPT Tip Resistance For Different Factors Of Safety (FS)

Generally, liquefaction-induced ground failure include flow slides, lateral spreads, ground settlements, ground oscillation, and sand boils. Lateral spreads are the pervasive types of liquefaction-induced ground failures for gentle slopes or for nearly level ground with free face

Lateral displacement index (LDI) is defines as follows:

$$LDI = \int_{0}^{Z_{max}} \gamma_{max}\, dz$$

Where

Z_{max} = maximum depth below all the potential liquefiable layers with a calculated SF < 2.0

γ_{max} = maximum cyclic shear strains

Where γ_{max} be approach by the following mathematical expressions:

if $D_r = 90\%$ $\gamma_{max} = 3.26(FS)^{-1.80}$ for 0.7≤SF≤2.0
if $D_r = 90\%$ $\gamma_{max} = 6.2$ for SF≤0.7
if $D_r = 80\%$ $\gamma_{max} = 3.22(FS)^{-2.08}$ for 0.56 ≤SF≤2.0
if $D_r = 80\%$ $\gamma_{max} = 10$ for SF≤0.56
if $D_r = 70\%$ $\gamma_{max} = 3.20(FS)^{-2.89}$ for 0.59 ≤SF≤2.0
if $D_r = 70\%$ $\gamma_{max} = 14.5$ for SF≤5.9
if $D_r = 60\%$ $\gamma_{max} = 3.58(FS)^{-4.42}$ for 0.66 ≤SF≤2.0
if $D_r = 60\%$ $\gamma_{max} = 22.7$ for SF≤0.66
if $D_r = 50\%$ $\gamma_{max} = 4.22(FS)^{-6.39}$ for 0.72 ≤SF≤2.0
if $D_r = 50\%$ $\gamma_{max} = 34.1$ for SF≤0.72
if $D_r = 40\%$ $\gamma_{max} = 3.31(FS)^{-7.97}$ for 1.0 ≤SF≤2.0
if $D_r = 40\%$ $\gamma_{max} = 250\,.(1.0 - FS) + 3.5$ for 0.81 ≤SF≤1.0
if $D_r = 40\%$ $\gamma_{max} = 51.2$ for SF≤0.81

Approach for Lateral Displacement (LD) is recommended for use based on the research mostly in Japan and America with its earthquake properties and ground condition, moment magnitude between 6.4 and 9.2, peak surface acceleration between 0.19 g and 0.6 g, and free face height less than 18 m (Juang, Ching, Wang, Khoshnevisan, & Ku, 2013). Lateral Displacement can be estimated with equation bellow:

LD = (S + 0.2) LDI

Where

LD =Lateral Displacement

S =Knowing ground slope

Figure 4 shows several locations in Mataram city in where soil data is being taken by using SPT or CPT. Most locations are being tested by either SPT or CPT and some are taken by both SPT and CPT. The earthquake profile is based on the 2018 M7.0.

Figure 5
Locations of Data SPT and CPT Taken

Results and Discussion

In this chapter of journal, results of factor of safety acquired from the calculations of CPT and CPT data in accordance to the depth of observation are depicted in Figure 6 to Figure 7.

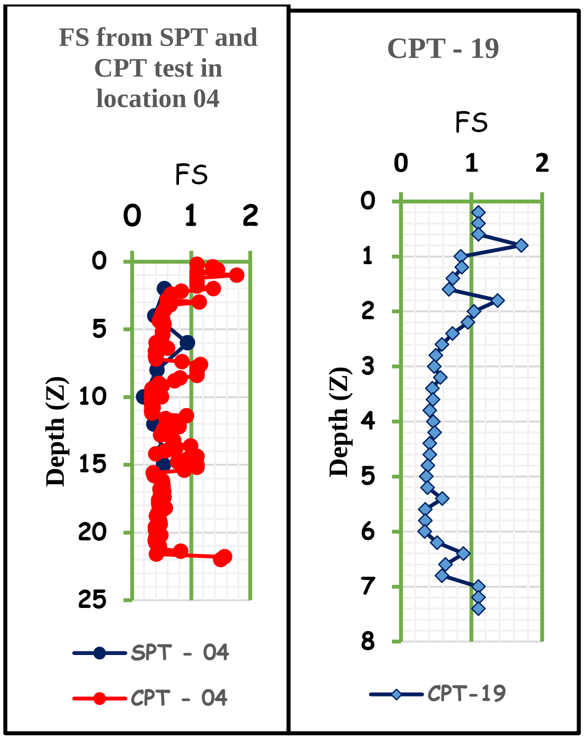

Figure 6
SF on Location 04 and 19 (Downtown and West Coast)

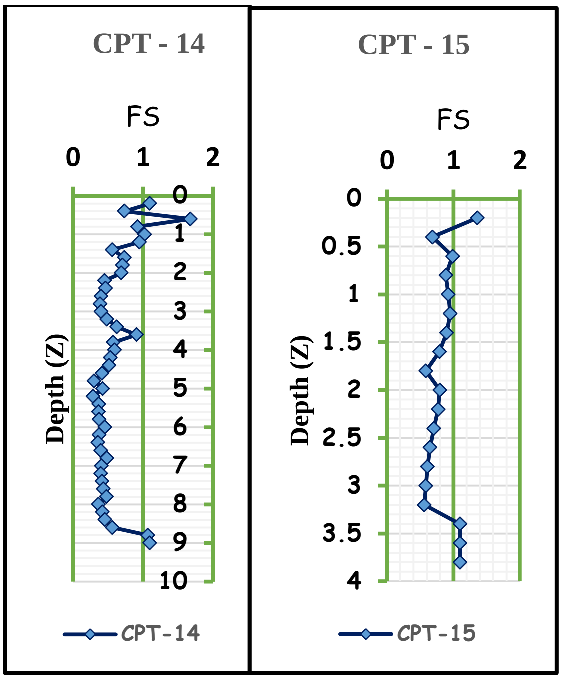

Figure 7
SF on Location 14 and 15 (North Area and Eastern Area)

Table 3
Recapitulation of Settlement and Lateral Displacement

Location	Coordinates	Depth (z) max	Σ I_L	Σ S	Max LD
		(m)		(m)	(m)
CPT - 01	-8.5777629 , 116.086348	16.8	35.62	0.35	0.015
CPT - 02	-8.5777486 , 116.0867196	22	31.70	0.40	0.010
CPT - 03	-8.5777486 , 116.0867196	22	31.40	0.40	0.010
CPT - 04	-8.5790728 , 116.0886944	22	32.30	0.10	0.010
CPT - 05	-8.6200626 , 116.0822933	8	13.58	0.09	0.010
CPT - 06	-8.6181029 , 116.1648509	9	16.81	0.10	0.0064
CPT - 07	-8.6176298 , 116.1649291	8.4	9.21	0.06	0.0064
CPT - 08	-8.6176298 , 116.1649291	6.6	13.40	0.09	0.0065
CPT - 09	-8.6055768 , 116.0904813	10.8	36.73	0.21	0.010
CPT - 10	-8.5733601 , 116.1022052	6	7.19	0.05	0.0064
CPT - 11	-8.5945499 , 116.102548	17.6	36.85	0.37	0.010
CPT - 12	-8.5971415 , 116.1601164	5.6	15.90	0.12	0.010
CPT - 13	-8.6194192 , 116.0975514	11.6	31.95	0.23	0.010
CPT - 14	-8.5664244 , 116.1131799	9	29.36	0.19	0.010
CPT - 15	-8.5927082 , 116.1559701	3.8	6.42	0.06	0.0064
CPT - 16	-8.5844697 , 116.1286235	12.4	22.0	0.21	0.010
CPT - 17	-8.5641529 , 116.0981165	14.4	37.12	0.28	0.010
CPT - 18	-8.5955247 , 116.1126641	8.6	13.22	0.10	0.0064
CPT - 19	-8.6003905 , 116.0836751	7.4	19.69	0.12	0.0064
CPT - 20	-8.5842564 , 116.1072639	12	16.51	0.14	0.010
CPT - 21	-8.5705941 , 116.728371	2	38.80	0.46	0.010
CPT - 22	-8.588308 , 116.1453149	4.8	6.29	0.05	0.010

Conclusion

Generally speaking, Mataram city is prone to liquefaction with most of the liquefaction potential may happen from at 2 meters below the surface. Figure 5 shows that downtown area is heavily prone to liquefaction starting from 2 meter below until more than 20 meter. While the west coast is also have a high potential of liquefaction according to Figure 5 and having the biggest settlement potential (0.46 m) according to data obtained on CPT-21. This may due to the its location close to the epicenter of the past earthquake and the location of most of rivers downstream, the place where most of the soil being soft. It shows a significant potential up to 20 m below. The same pattern is also observed on the northern part of the city, where the FS < 1 is commonly observed from 2 m up until 13 m. Nevertheless, it shows a smaller magnitude compared to that of the western coast.

Moreover, the eastern part shows the least potential of liquefaction as shown in Figure 6 and the least settlement potential on only 0.05 m obtained at CPT-22 site. This can happen due to the higher altitude and the presence of strong soil in the surrounding area. Lastly, the southern part of the city indicates a relatively medium potential of liquefaction, although it is worth noticing the effect of liquefaction might increase due to its close location to the west sites. Finally, looking at the calculation results, it is can be concluded that Mataram city has a high potential of liquefaction and it is recommended to take a further actions.

BIBLIOGRAFI

Aryastana, Putu, Ardantha, I., Eka Nugraha, Adrianto, & Windy Candrayana, Kadek. (2017). *Coastline changes analysis in Buleleng regency by using satellite data*. Google Scholar

Blake, T. F. (1996). Spreadsheet Template LIQ2_30. *WQ1-A Computer Program for the Determination of Liquefaction Potential*. Google Scholar

Castelli, Francesco, & Lentini, Valentina. (2010). SPT-based evaluation of soil liquefaction risk. *Fifth International Conference on Recent Advances in Geotechnical Earthquake Engineering and Soil Dynamics*. Google Scholar

Green, Russell A., Upadhyaya, Sneha, Wood, Clinton M., Maurer, Brett W., Cox, Brady R., Wotherspoon, Liam, Bradley, Brendon A., & Cubrinovski, Misko. (2017). Relative efficacy of CPT-versus Vs-based simplified liquefaction evaluation procedures. *Proc. 19th Intern. Conf. on Soil Mechanics and Geotechnical Engineering*, 1521–1524. Google Scholar

Jefferies, Mike, & Been, Ken. (2019). *Soil liquefaction: a critical state approach*. CRC press. Google Scholar

Juang, C. Hsein, Ching, Jianye, Wang, Lei, Khoshnevisan, Sara, & Ku, Chih Sheng. (2013). Simplified procedure for estimation of liquefaction-induced settlement and site-specific probabilistic settlement exceedance curve using cone penetration test (CPT). *Canadian Geotechnical Journal*, *50*(10), 1055–1066. Google Scholar

Lonteng, Christian Vicky Delfis, Balamba, Sjachrul, Monintja, Sartje, & Sarajar, Alva N. (2013). Analisis Potensi Likuifaksi Di PT. Pln (Persero) Uip Kit Sulmapa Pltu 2 Sulawesi Utara 2 X 25 Mw Power Plan. *Jurnal Sipil Statik*, *1*(11). Google Scholar

Obermeier, Stephen F. (1996). Use of liquefaction-induced features for paleoseismic analysis—an overview of how seismic liquefaction features can be distinguished from other features and how their regional distribution and properties of source sediment can be used to infer the location and strength of Holocene paleo-earthquakes. *Engineering Geology*, *44*(1–4), 1–76. Google Scholar

Putra, Rusnardi Rahmat, Kiyono, Junji, Ono, Yusuke, & Parajuli, Hari Ram. (2012). Seismic hazard analysis for Indonesia. *Journal of Natural Disaster Science*, *33*(2), 59–70. Google Scholar

Robertson, Peter K. (2016). Cone penetration test (CPT)-based soil behaviour type (SBT) classification system—an update. *Canadian Geotechnical Journal*, *53*(12), 1910–1927. Google Scholar

Sasmi, Annisa Trisnia, Nugraha, Andri Dian, Muzli, Muzli, Widiyantoro, Sri, Zulfakriza, Zulfakriza, Wei, Shengji, Sahara, David P., Riyanto, Agus, Puspito, Nanang T., & Priyono, Awali. (2020). Hypocenter and magnitude analysis of aftershocks of the 2018 Lombok, Indonesia, earthquakes using local seismographic networks. *Seismological Research Letters*, *91*(4), 2152–2162. Google Scholar

Saut, Pantas O. Siahaan. (2015). *Percobaan Potensi Likuifaksi Pada Tanah Pasir Seragam Dengan Permodelan Alat Di Laboratorium*. UPT. Perpustakaan Unand. Google Scholar

Tijow, Kurnia Christy, Sompie, Oktovian B. A., & Ticoh, Jack H. (2018). Analisis Potensi Likuifaksi Tanah Berdasarkan Data Standart Penetration Test (Spt) Studi Kasus: Dermaga Bitung, Sulawesi Utara. *Jurnal Sipil Statik*, *6*(7). Google Scholar

Warman, Hendri, & Jumas, Dwifitria Y. (2013). Kajian Potensi Likuifaksi Pasca Gempa Dalam Rangka Mitigasi Bencana di Padang. *Jurnal Rekayasa Sipil (JRS-Unand)*, *9*(2), 1–19. Google Scholar

Youd, T. Leslie, & Idriss, Izzat M. (2001). Liquefaction resistance of soils: summary report from the 1996 NCEER and 1998 NCEER/NSF workshops on evaluation of liquefaction resistance of soils. *Journal of Geotechnical and Geoenvironmental Engineering*, *127*(4), 297–313. Google Scholar

Zhang, G., Robertson, P. K., & Brachman, R. W. I. (2002). Estimating liquefaction-induced ground settlements from CPT for level ground. *Canadian Geotechnical Journal*, *39*(5), 1168–1180. Google Scholar

Copyright holder:
Intan Puspitaningrum (2021)

First publication right:
Syntax Literate: Jurnal Ilmiah Indonesia

This article is licensed under: